Letter | Editors' Suggestion

Strain control of exciton and trion spin-valley dynamics in monolayer transition metal dichalcogenides

Z. An,[1,*] P. Soubelet,[2,*,†] Y. Zhumagulov,[3] M. Zopf,[1,‡] A. Delhomme,[2] C. Qian,[2] P. E. Faria Junior,[3] J. Fabian,[3] X. Cao,[1] J. Yang,[1] A. V. Stier,[2] F. Ding,[1] and J. J. Finley[2]

[1]*Institute of Solid State Physics, Leibniz Universität Hannover, Appelstraße 2, 30167 Hannover, Germany*

[2]*Walter Schottky Institut and TUM School of Natural Sciences, Technische Universität München, Am Coulombwall 4, 85748 Garching, Germany*

[3]*Institute for Theoretical Physics, University of Regensburg, 93040 Regensburg, Germany*

(Received 28 March 2023; accepted 13 June 2023; published 20 July 2023)

The electron-hole exchange interaction is a fundamental mechanism that drives valley depolarization via intervalley exciton hopping in semiconductor multivalley systems. Here, we report polarization-resolved photoluminescence spectroscopy of neutral excitons and negatively charged trions in monolayer $MoSe_2$ and WSe_2 under biaxial strain. We observe a marked enhancement (reduction) on the WSe_2 triplet trion valley polarization with compressive (tensile) strain while the trion in $MoSe_2$ is unaffected. The origin of this effect is shown to be a strain-dependent tuning of the electron-hole exchange interaction. A combined analysis of the strain-dependent polarization degree using *ab initio* calculations and rate equations shows that strain affects intervalley scattering beyond what is expected from strain-dependent band-gap modulations. The results evidence how strain can be used to tune valley physics in energetically degenerate multivalley systems.

DOI: 10.1103/PhysRevB.108.L041404

Semiconducting transition metal dichalcogenides (TMDs) are layered materials with strong light-matter interactions. In the monolayer (ML) limit, they are direct band-gap materials [1,2] at the K/K' points of their hexagonal Brillouin zone [3], where interband optical transitions form tightly bound excitons [4–8]. Furthermore, strong spin-orbit coupling (SOC) and the inherently broken inversion symmetry couples spin- and valley degrees of freedom causing chiral optical selection rules with marked valley dichroism [9–16]. Based on initial first-principles calculations that predicted long valley coherence times [17,18] and the possibility to coherently control this pseudospin [14,15,19–23], the concept of valleytronics was envisioned as a promising route to process and store information. However, short exciton lifetimes, fast decoherence, and fast valley depolarization limit practical applications of two-dimensional (2D) TMDs for valleytronics [12,18,24–26]. While different approaches have been pursued to investigate valley depolarization in TMDs, significant variations in the valley depolarization times from a few picoseconds (ps) [18,27–29] to several tens of ps [18,30–32] have been observed, highlighting the continued need for a deeper understanding of the underlying valley physics. Of particular interest are the various electron-electron and electron-hole interaction channels in optically bright and dark ML TMDs [33–35].

At cryogenic temperatures, valley depolarization in semiconductor multivalley systems is mainly driven by electron-hole exchange interaction (EHEI) [19,22,26,30,36–38]. This mechanism, depicted schematically by its Feynman diagram for TMDs in Fig. 1(a), describes the Coulomb interaction between an electron in the conduction band (CB) at K, with an electron in the valence band (VB) at K'. As a result, the electron in the CB at K is scattered to the VB at K while the electron in the VB of K' is scattered to the CB at K' [26]. Effectively, the EHEI results in the annihilation of a bright exciton at K and the creation of a bright exciton at K'. The effect of the EHEI markedly depends on the TMD band structure and exciton configurations [20,33]. For instance, in ML molybdenum-diselenide ($MoSe_2$), adding an electron to the neutral exciton limits the EHEI and protects trions from intervalley scattering, reducing trion valley depolarization [12,39]. In contrast, negatively charged trions in tungsten diselenide (WSe_2) are split into the *intervalley* triplet trion (T_t) and the *intravalley* singlet trion (T_s) configurations [40,41], allowing electron-hole pair hopping from K to K' through triplet-to-singlet conversion [42].

In this Letter, we use piezoelectric devices to apply biaxial strain (s) to ML WSe_2 and $MoSe_2$ at cryogenic temperatures [43–46] and investigate the valley depolarization of excitons and negatively charged trions. Although strain engineering was broadly used in 2D materials to study modulations of the band gap and vibrational modes [43–57], the effect of strain on the valley depolarization was studied theoretically [58,59] and only a few experimental realizations were performed trough uniaxial strain at room temperature [60] or via nontunable devices [61]. By performing circularly polarized photoluminescence (PL) spectroscopy as a function of s, we observe that while negative trions in $MoSe_2$ are not affected, triplet trions in WSe_2 strongly valley depolarize. *Ab initio*

*These authors contributed equally to this work.
†pedro.soubelet@wsi.tum.de
‡michael.zopf@fkp.uni-hannover.de

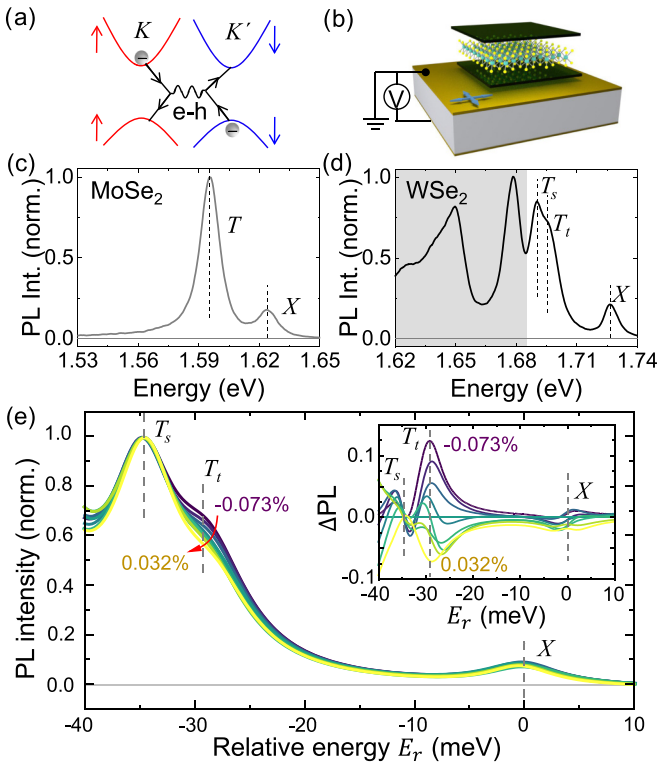

FIG. 1. (a) Feynman diagram of the bright exciton transition between K and K' due to EHEI. A spin-up electron in the CB at K and a spin-down electron in the VB at K' are scattered to their final states in the VB at K and the CB at K', respectively. (b) Schematic of the sample stack: piezoelectric substrate, its electric connections, and the hBN-encapsulated ML TMD. Microphotoluminescence (μPL) spectra at 10 K of the (c) ML $MoSe_2$ and (d) WSe_2. The $MoSe_2$ spectra show the X and T emission. In WSe_2, the spectra display the X, the triplet (T_t), and the singlet (T_s) trion. Emissions at lower energy (gray shade) are outside the scope of this Letter. (e) WSe_2 PL for s ranging from -0.073% to 0.032%. Energy scale is relative to X and spectra are normalized to the T_s emission intensity. Inset: Differential PL (ΔPL) showing the variation of the PL with respect to the emission at $s = 0$.

calculations show that s predominantly affects the EHEI and therefore the intervalley scattering time via the modulation of the band gap. Using these results, we model the strain-dependent exciton/trion polarization with rate equations that consider the interplay between the exciton/trion radiative lifetime and the intervalley scattering time. Although we find qualitative agreement between experiments and theory, the experimentally observed variation of the exciton/trion depolarization is notably stronger. Our observations, therefore, suggest the use of s as an efficient way to control exciton and trion valley dynamics while maintaining K/K' degeneracy.

Results and discussion. The strain actuators are piezoelectric crystals of lead magnesium niobate–lead titanate (PMN-PT) [62] with electrical top/bottom gold contacts. Biaxial strain at cryogenic temperatures (10 K) is applied to the ML TMDs stack by poling the PMN-PT crystal with a constant voltage V across the piezoelectric element, as shown in Fig. 1(b) [43–46]. The ML TMDs were obtained from commercial bulk crystals through mechanical exfoliation. The ML TMDs were subsequently encapsulated between thin hexagonal boron nitride (hBN) by using dry transfer techniques based on polycarbonate films, similar to Ref. [63]. The assembled structure was stamped directly on top of the piezoelectric substrates. Special care was taken to ground the top electrode of the piezoelectric element to prevent unintentional charging of the TMDs during the experiments. Details about the strain devices are presented in Sec. I of the Supplemental Material (SM) [64] (see also Refs. [43–45,62,65–67]).

Photoluminescence spectra were recorded at the center of each ML TMD with an optical cw power $P = 1$ μW focused to a diffraction limited spot [100× objective, numerical aperture (NA) = 0.7]. The samples were excited at $E_P = 1.96$ eV for WSe_2 and $E_P = 1.68$ eV for $MoSe_2$. All data shown in this Letter were found to be strain reversible and the experiments in the WSe_2 case were repeated in a second sample (see SM Secs. I and II [64]). Representative PL spectra for the samples at zero applied strain are shown in Figs. 1(c) and 1(d). The emission feature at ∼1.623 eV (∼1.728 eV) for $MoSe_2$ (WSe_2) is associated with the neutral bright exciton (X), consistent with previous studies for hBN-encapsulated ML TMDs [68–71]. The $MoSe_2$ spectrum shows an additional single peak ∼30 meV red detuned from the X emission and consistent with negative trions (T) of the *intervalley* singlet type [20,70,72]. Conversely, WSe_2 shows the singlet (T_s) and the triplet (T_t) trion at ∼1.686 and ∼1.692 eV, respectively, in agreement with previous reports [20,41,73–77]. In addition, we observe the emission from localized states and phonon replicas (gray shade) as described in Ref. [74]. We do not discuss these features further in the remainder of this Letter, since they are not central to the studied photophysics. From the relative T/X emission intensity and peak positions, we estimate an electron density $n_e(MoSe_2) = 2.5 \times 10^{10}$ cm^{-2} and $n_e(WSe_2) = 3 \times 10^{11}$ cm^{-2} in our samples [70,75].

We continue by describing the effect of s on the emission energy and intensity of excitons and trions. By varying the voltage applied to the piezoelectric element, from −400 to 400 V, the neutral exciton emission of both materials continuously blueshifts by ∼10 meV, consistent with a total strain variation of $\Delta s \sim 0.1\%$ across the voltage range [78]. Details about the method used to calibrate s are shown in Sec. II of the SM [64]. We performed first-principles calculations in the range of the experimentally applied strain to confirm that the band gap is mainly affected, whereas changes in the effective masses, spin mixing, electron-electron interactions [79], and interband dipole matrix elements are negligible. For the interested reader, these calculated quantities are summarized in Sec. IV of the SM [64] (see also Refs. [78,80–84]).

The effect of strain on the X/T emission intensity is presented in Fig. 1(e), where we plot the copolarized PL spectra (σ^+ excitation and collection) of the WSe_2 sample for various strains. All spectra are normalized to the singlet trion intensity and the energy axis relative to the X energy (E_X) [85]. T_s and X emission intensities are approximately constant (see SM Sec. I for details [64]), consistent with a picture where the exciton generation rate and recombination time are not affected by the small amount of s exerted by the piezoelectric device. However, the triplet trion shows a relative decrease of its intensity by increasing s. The inset in Fig. 1(e) shows the differential PL

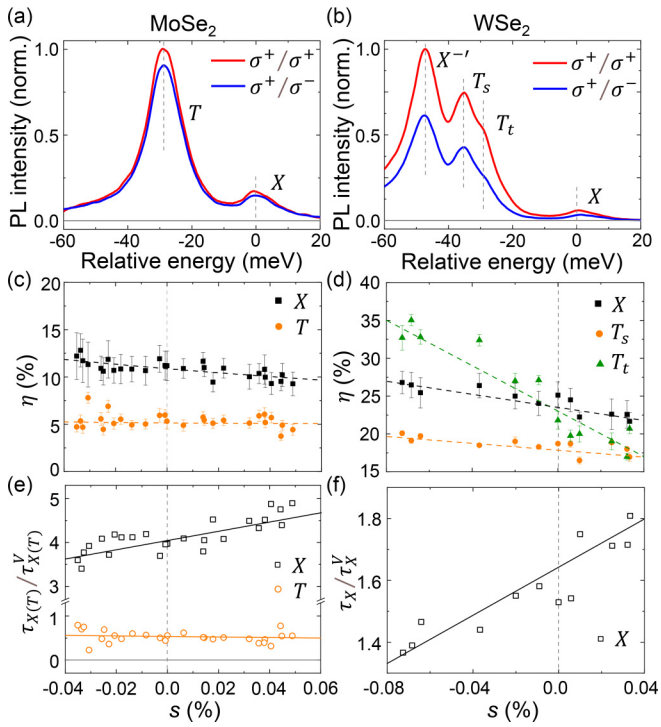

FIG. 2. Polarization-resolved μPL spectra for (a) ML $MoSe_2$ and (b) WSe_2 at $s = 0$. Red (blue) spectra are obtained for σ^+ excitation and σ^+ (σ^-) detection. The energy scale is relative to the X and spectra are normalized to the feature with the highest intensity in the copolarized configuration. (c) η_X (black) and η_T (orange) for ML $MoSe_2$ as a function of s. (d) Neutral exciton (black), singlet trion (orange), and triplet trion (green) circular polarization degree as a function of s for ML WSe_2. Dashed lines in (c) and (d) are guides to the eye. (e) Ratio of total decay rate (τ) to the total intervalley scattering rate (τ^V) for excitons (black dots) and trions (orange dots) in $MoSe_2$. (f) Ratio of τ/τ^V as a function of s for excitons in WSe_2. Solid lines in (e) and (f) are linear fits to the data.

[ΔPL = PL(s) − PL($s = 0$)], further highlighting the effect of s on the T_t emission. This experiment shows that the relative intensities between trions is not only sensitive to the electron background density in the sample [74,75,86] but also to the local strain.

To further investigate the strain response of T_t, we perform polarization-resolved PL as a function of strain on both materials. The spectra at $s = 0$ are shown in Figs. 2(a) and 2(b) for $MoSe_2$ and WSe_2, respectively. Red (blue) correspond to σ^+ excitation and σ^+ (σ^-) collection. In both cases, the energy scale is relative to E_X and the spectra are normalized to the σ^+ PL intensity of T for $MoSe_2$ or the peak labeled as $X^{-'}$ for WSe_2 [74]. The significant cross-polarized PL intensity suggests a strong valley depolarization mechanism, particularly for $MoSe_2$. We characterize this effect by means of the circular polarization degree (η) calculated for each feature, $\eta_x = (I_x^+ - I_x^-)/(I_x^+ + I_x^-)$, where x labels the feature (exciton or trion) and I_x^+ (I_x^-) are co- (cross-)polarized intensities obtained by Lorentzian fits to the data. We provide additional information about this procedure in Sec. II of the SM [64].

Figure 2(c) shows η_X and η_T as a function of s for $MoSe_2$ and Fig. 2(d) η_X, η_{T_s}, and η_{T_t} for WSe_2. The difference between these two materials as well as the different behavior of excitons and trions are the main experimental observations of this Letter. For $MoSe_2$, η_X shows a small but clear variation of ∼2% while η_T is constant within our experimental error. For WSe_2, η_X and η_{T_s} vary similarly by ∼5% while η_{T_t} shows a much stronger response, changing by ∼15% over the whole range of strain investigated. Though these values depend on the excitation power, the general trends are independent of the laser intensity (see SM Sec. II [64]). The error bars given in Figs. 2(c) and 2(d) take the mathematical error of the fitting routine and the polarization accuracy of our setup (∼98%) into account.

To understand the strain-dependent η, we model the system by rate equations, considering the strain-dependent recombination times (τ_X and τ_T for X and T, respectively) and valley scattering times (τ_X^V for X and τ_T^V for T). In the linear regime, η_X is given by (see Ref. [15] and SM Sec. III [64])

$$\eta_X = \frac{\eta_{X0}}{1 + 2\tau_X/\tau_X^V}, \tag{1}$$

where η_{X0} is the spin polarization at the instance of generation. Although the absolute value of η_{X0} (and therefore η_X) depends on the *excess energy* $\Delta E = (E_P - E_X)/2$ [58,87,88], it is a proportionality factor and does not affect the general trend we attempt to describe. Therefore, we assume $\eta_{X0} = 1$ in the following discussion. By combining Eq. (1) with the η_X data [Figs. 2(c) and 2(d)], we calculate the ratio τ_X/τ_X^V, shown in black squares in Figs. 2(e) and 2(f) for $MoSe_2$ and WSe_2, respectively. Solid lines are linear fits that yield the strain dependence of τ_X/τ_X^V as $(10 \pm 2)/\%$ for $MoSe_2$ and $(4 \pm 1)/\%$ for WSe_2, i.e., similar relative variation in both cases.

We continue by describing the strain-dependent valley depolarization of trions. For trions in $MoSe_2$, we use the same assumptions as for excitons, which results in (see Ref. [15] and SM Sec. III [64])

$$\eta_T = \frac{\eta_X}{1 + 2\tau_T/\tau_T^V}. \tag{2}$$

Note that as trions require the existence of an exciton, the trion polarization at the instance of generation is η_X. Once again, by combining Eq. (2) with the $\eta(s)$ data in Fig. 2(c), we obtain the ratio τ_T/τ_T^V shown as orange circles in Fig. 2(e). The ratio $\tau_T/\tau_T^V < 1$ denotes a comparatively shorter recombination time and a minor influence of the intervalley scattering in the trion dynamics.

Comparing the ratio τ_X/τ_X^V in both materials, τ_X/τ_X^V is approximately 2.5× larger in $MoSe_2$ than in WSe_2. This is consistent with a relatively faster exciton intervalley scattering in $MoSe_2$, which is anticipated due to an additional depolarization mechanisms, such as the Rashba-type mixing of bright and dark excitons [35]. In Ref. [58], the authors calculated η_X by a two-band $k \cdot p$ method and found that $\Delta E > 0$ provides a strain-dependent valley depolarization. Nevertheless, the strain-induced depolarization we observe is two orders of magnitude larger than their prediction, suggesting a different cause. While τ_X/τ_X^V depends on strain in both materials, τ_T/τ_T^V in $MoSe_2$ is constant across the strain range [Figs. 2(e)

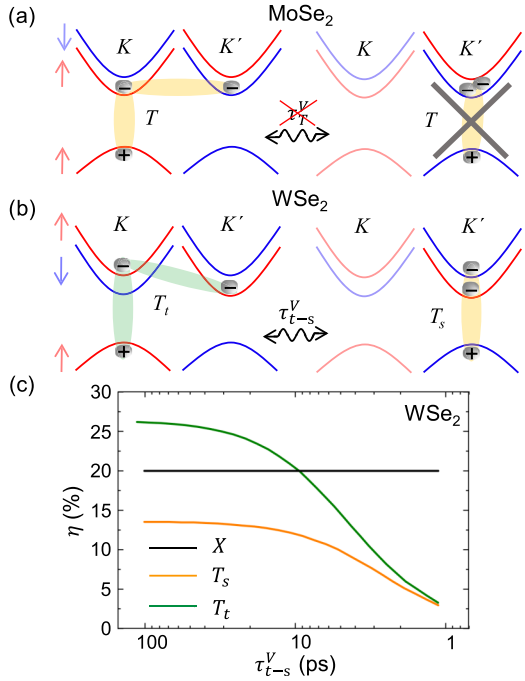

FIG. 3. Sketch of the intervalley scattering effects in monolayer TMDs. (a) $MoSe_2$ trions are spin protected against EHEI. (b) In WSe_2, EHEI transforms triplet trions at K into singlet trions at K'. (c) Calculated η_X (black), η_{T_s} (orange) and η_{T_t} (green) as a function of trion intervalley scattering time τ^V_{t-s} in WSe_2.

and 2(f)]. On the other hand, singlet and triplet trions in WSe_2 depolarize in the same strain range [Fig. 2(d)]. We consider that the only possible explanation for these different behaviors is that s is able to tune the EHEI. Therefore, τ_T/τ^V_T in $MoSe_2$ is independent of strain due to the lack of EHEI for trions since they are spin protected [23,72] [see Fig. 3(a)]. In WSe_2, instead, the EHEI allows intervalley scattering through a triplet-to-singlet conversion, as sketched in Fig. 3(b) [42]. Consequently, we interpret our strain-dependent trion data through a triplet-to-singlet conversion mediated by a strain-dependent EHEI.

The addition of the triplet-to-singlet conversion scattering channel in the rate equations model is characterized by introducing the scattering time τ^V_{t-s}, which renders the solution nonanalytical (see SM Sec. III [64]). As the singlet-to-triplet scattering term is proportional to the difference of the singlet and triplet population, the resulting populations are interdependent. For this reason the ratio between trion lifetime and intervalley scattering is not the only variable that defines the trion polarization degree in WSe_2 and cannot be extracted from the equations as in $MoSe_2$. We numerically solve the rate equations and plot in Fig. 3(c) the values obtained for η_X, η_{T_s}, and η_{T_t} using a fixed set of realistic input parameters ($\tau_X = 1$ ps, $\tau_{T_t} = 2$ ps, $\tau_{T_s} = 4$ ps, $\tau^V_X = 0.5$ ps, and trion formation time $\tau_b = 0.1$ ps) while sweeping τ^V_{t-s}. By decreasing τ^V_{t-s}, the singlet-to-triplet conversion starts to dominate the intervalley dynamics and $\eta_{T_{s,t}}$ decrease with a markedly different slope ultimately tending to zero. When $\tau^V_{t-s} \sim 10$ ps our rate equations reproduce the experimentally observed $\eta(s)$ very well [see Fig. 2(d)].

To test our assumption, we model the strain-dependent exciton radiative decay rates and intervalley EHEI scattering times from first principles (see SM Sec. IV [64] and Refs. [14,22,40,41,71,86,89–92]). Our calculations show that the radiative decay time is barely strain dependent. Conversely, the EHEI strongly depends on the band gap, which shrinks with tensile strain. Consequently, the EHEI scattering time markedly decreases by increasing tensile strain. Both observations are consistent with the general trends of our experimentally determined polarization results, however, the strain dependence we observe is an order of magnitude larger than our calculations. As the small amount of strain applied in the experiments affects the TMDs band gap but not their band structure (see SM Sec. IV [64] and Refs. [78,80–84]), any other channel for recombination and intervalley scattering is treated as a constant background without affecting our results.

Finally, we note that in Ref. [75], the authors propose a mechanism based on the spin-valley pumping of resident *electrons* for tungsten composite TMDs that leads to a pump- and doping-dependent $\eta_{T_{s,t}}$. This effect results from an efficient phonon-mediated scattering of electrons from the upper CB in K to the lower CB in K'. For a single pump power, we note that we can interpret our trion results based on this effect by introducing a strain-dependent *electron* intervalley scattering time in our rate equations. However, our observations for *excitons* in both materials can only be explained by a strain-dependent EHEI.

In summary, we observe clear experimental evidence of a strain-dependent EHEI, supported by first-principles calculations. We presented a detailed study of the biaxial strain impact on the circular polarization degree of excitons and trions in $MoSe_2$ and WSe_2. The circular polarization degree depends on the total exciton and trion lifetimes and their depolarization rates [15]. While the radiative decay is essentially independent of strain, the strain-dependent intervalley scattering is the only consistent way to explain our observations on $\eta(s)$. This suggests that strain modulates the EHEI to a surprisingly large degree beyond expectations from first-principles calculations that only take a strain-dependent band gap into account. Our observations may consolidate the variations of optical polarization degrees and intervalley scattering times reported in the literature and point towards a scattering channel besides the occurrence of resident electrons that facilitates valley depolarization, such as the mixing of singlet and triplet trion states [93]. Our results highlight the need for further understanding of the spin/valley photophysics in TMDs and point out a possible path to enhance valley polarization towards the development of valleytronics in multivalley materials.

We gratefully acknowledge the German Science Foundation (DFG) for financial support via SPP-2244 grants (DI 2013/5-1, FI 947/8-1, and FA 971/8-1). P.S., A.D., C.Q., A.V.S., and J.J.F. additionally acknowledge the clusters of excellence MCQST (EXS-2111) and e-conversion (EXS-2089). Z.A., M.Z., X.C., J.Y., and F.D. gratefully acknowledge the European Research Council (No. QD-NOMS GA715770), and the DFG Excellence Strategy-EXC-2123 Quantum Frontiers-39083 7967. Z.A. is funded by the China Scholarship Council. Y.Z., P.E.F.J., and J.F. also

acknowledge the financial support of the DFG SFB 1277 (Project-ID 314695032, projects B07 and B11).

A.V.S., F.D., and J.J.F. conceived the project. P.S. and C.Q. prepared the samples, Z.A. and P.S. performed the optical measurements on WSe_2, and P.S. and A.D. on $MoSe_2$. Z.A., M.Z., X.C., and J.Y. provided support on the piezoelectric performance, and M.Z., X.C., and J.Y. supervised the experiments performed in Hannover. Y.Z., P.E.F.J., and J.F. provided support on the theory and *ab initio* calculations. P.S. and Z.A. analyzed the data and P.S. and Y.Z. developed the rate equation model. P.S. wrote the paper with input from all coauthors. All authors reviewed the manuscript.

The authors declare no competing financial or nonfinancial interests.

[1] K. F. Mak, C. Lee, J. Hone, J. Shan, and T. F. Heinz, Phys. Rev. Lett. **105**, 136805 (2010).
[2] A. Splendiani, L. Sun, Y. Zhang, T. Li, J. Kim, C.-Y. Chim, G. Galli, and F. Wang, Nano Lett. **10**, 1271 (2010).
[3] D. Xiao, G.-B. Liu, W. Feng, X. Xu, and W. Yao, Phys. Rev. Lett. **108**, 196802 (2012).
[4] K. F. Mak, K. He, C. Lee, G. H. Lee, J. Hone, T. F. Heinz, and J. Shan, Nat. Mater. **12**, 207 (2013).
[5] A. Chernikov, T. C. Berkelbach, H. M. Hill, A. Rigosi, Y. Li, Ö. B. Aslan, D. R. Reichman, M. S. Hybertsen, and T. F. Heinz, in *2014 Conference on Lasers and Electro-Optics (CLEO)-Laser Science to Photonic Applications* (IEEE, New York, 2014), pp. 1 and 2.
[6] A. V. Stier, K. M. McCreary, B. T. Jonker, J. Kono, and S. A. Crooker, Nat. Commun. **7**, 10643 (2016).
[7] A. V. Stier, N. P. Wilson, K. A. Velizhanin, J. Kono, X. Xu, and S. A. Crooker, Phys. Rev. Lett. **120**, 057405 (2018).
[8] M. Goryca, J. Li, A. V. Stier, T. Taniguchi, K. Watanabe, E. Courtade, S. Shree, C. Robert, B. Urbaszek, X. Marie *et al.*, Nat. Commun. **10**, 4172 (2019).
[9] O. Gunawan, Y. P. Shkolnikov, K. Vakili, T. Gokmen, E. P. De Poortere, and M. Shayegan, Phys. Rev. Lett. **97**, 186404 (2006).
[10] X. Xu, W. Yao, D. Xiao, and T. F. Heinz, Nat. Phys. **10**, 343 (2014).
[11] K. F. Mak, D. Xiao, and J. Shan, Nat. Photonics **12**, 451 (2018).
[12] J. R. Schaibley, H. Yu, G. Clark, P. Rivera, J. S. Ross, K. L. Seyler, W. Yao, and X. Xu, Nat. Rev. Mater. **1**, 16055 (2016).
[13] G. Sallen, L. Bouet, X. Marie, G. Wang, C. R. Zhu, W. P. Han, Y. Lu, P. H. Tan, T. Amand, B. L. Liu, and B. Urbaszek, Phys. Rev. B **86**, 081301(R) (2012).
[14] T. Cao, G. Wang, W. Han, H. Ye, C. Zhu, J. Shi, Q. Niu, P. Tan, E. Wang, B. Liu, and J. Feng, Nat. Commun. **3**, 887 (2012).
[15] K. F. Mak, K. He, J. Shan, and T. F. Heinz, Nat. Nanotechnol. **7**, 494 (2012).
[16] H. Zeng, J. Dai, W. Yao, D. Xiao, and X. Cui, Nat. Nanotechnol. **7**, 490 (2012).
[17] G.-B. Liu, W.-Y. Shan, Y. Yao, W. Yao, and D. Xiao, Phys. Rev. B **88**, 085433 (2013).
[18] C. R. Zhu, K. Zhang, M. Glazov, B. Urbaszek, T. Amand, Z. W. Ji, B. L. Liu, and X. Marie, Phys. Rev. B **90**, 161302(R) (2014).
[19] G. Wang, X. Marie, B. L. Liu, T. Amand, C. Robert, F. Cadiz, P. Renucci, and B. Urbaszek, Phys. Rev. Lett. **117**, 187401 (2016).
[20] G. Wang, A. Chernikov, M. M. Glazov, T. F. Heinz, X. Marie, T. Amand, and B. Urbaszek, Rev. Mod. Phys. **90**, 021001 (2018).
[21] R. Schmidt, A. Arora, G. Plechinger, P. Nagler, A. Granados del Águila, M. V. Ballottin, P. C. M. Christianen, S. Michaelis de Vasconcellos, C. Schüller, T. Korn, and R. Bratschitsch, Phys. Rev. Lett. **117**, 077402 (2016).
[22] K. Hao, G. Moody, F. Wu, C. K. Dass, L. Xu, C.-H. Chen, L. Sun, M.-Y. Li, L.-J. Li, A. H. MacDonald *et al.*, Nat. Phys. **12**, 677 (2016).
[23] K. Hao, L. Xu, F. Wu, P. Nagler, K. Tran, X. Ma, C. Schüller, T. Korn, A. H. MacDonald, G. Moody *et al.*, 2D Mater. **4**, 025105 (2017).
[24] C. Robert, D. Lagarde, F. Cadiz, G. Wang, B. Lassagne, T. Amand, A. Balocchi, P. Renucci, S. Tongay, B. Urbaszek *et al.*, Phys. Rev. B **93**, 205423 (2016).
[25] G. Moody, J. Schaibley, and X. Xu, J. Opt. Soc. Am. B **33**, C39 (2016).
[26] T. Yu and M. W. Wu, Phys. Rev. B **89**, 205303 (2014).
[27] R. Schmidt, G. Berghauser, R. Schneider, M. Selig, P. Tonndorf, E. Malic, A. Knorr, S. Michaelis de Vasconcellos, and R. Bratschitsch, Nano Lett. **16**, 2945 (2016).
[28] J. Huang, T. B. Hoang, T. Ming, J. Kong, and M. H. Mikkelsen, Phys. Rev. B **95**, 075428 (2017).
[29] S. Dal Conte, F. Bottegoni, E. A. A. Pogna, D. De Fazio, S. Ambrogio, I. Bargigia, C. D'Andrea, A. Lombardo, M. Bruna, F. Ciccacci *et al.*, Phys. Rev. B **92**, 235425 (2015).
[30] T. Yan, X. Qiao, P. Tan, and X. Zhang, Sci. Rep. **5**, 15625 (2015).
[31] D. Lagarde, L. Bouet, X. Marie, C. R. Zhu, B. L. Liu, T. Amand, P. H. Tan, and B. Urbaszek, Phys. Rev. Lett. **112**, 047401 (2014).
[32] G. Plechinger, P. Nagler, A. Arora, R. Schmidt, A. Chernikov, A. G. Del Águila, P. C. Christianen, R. Bratschitsch, C. Schüller, and T. Korn, Nat. Commun. **7**, 12715 (2016).
[33] A. Kormányos, G. Burkard, M. Gmitra, J. Fabian, V. Zólyomi, N. D. Drummond, and V. Fal'ko, 2D Mater. **2**, 022001 (2015).
[34] P. Li, C. Robert, D. Van Tuan, L. Ren, M. Yang, X. Marie, and H. Dery, Phys. Rev. B **106**, 085414 (2022).
[35] M. Yang, C. Robert, Z. Lu, D. Van Tuan, D. Smirnov, X. Marie, and H. Dery, Phys. Rev. B **101**, 115307 (2020).
[36] Z. Ye, D. Sun, and T. F. Heinz, Nat. Phys. **13**, 26 (2017).
[37] A. K. Pattanayak, P. Das, A. Dhara, D. Chakrabarty, S. Paul, K. Gurnani, M. M. Brundavanam, and S. Dhara, Nano Lett. **22**, 4712 (2022).
[38] M. Z. Maialle, E. A. de Andrada e Silva, and L. J. Sham, Phys. Rev. B **47**, 15776 (1993).
[39] H. Yu, G.-B. Liu, P. Gong, X. Xu, and W. Yao, Nat. Commun. **5**, 3876 (2014).
[40] E. Courtade, M. Semina, M. Manca, M. M. Glazov, C. Robert, F. Cadiz, G. Wang, T. Taniguchi, K. Watanabe, M. Pierre, W. Escoffier, E. L. Ivchenko, R. Renucci, X. Marie, T. Amand, and B. Urbaszek, Phys. Rev. B **96**, 085302 (2017).

[41] J. Zipfel, K. Wagner, J. D. Ziegler, T. Taniguchi, K. Watanabe, M. A. Semina, and A. Chernikov, J. Chem. Phys. **153**, 034706 (2020).

[42] Y. V. Zhumagulov, A. Vagov, D. R. Gulevich, and V. Perebeinos, Nanomaterials **12**, 3728 (2022).

[43] J. Martín-Sánchez, R. Trotta, A. Mariscal, R. Serna, G. Piredda, S. Stroj, J. Edlinger, C. Schimpf, J. Aberl, T. Lettner *et al.*, Semicond. Sci. Technol. **33**, 013001 (2018).

[44] O. Iff, D. Tedeschi, J. Martín-Sánchez, M. Moczała-Dusanowska, S. Tongay, K. Yumigeta, J. Taboada-Gutiérrez, M. Savaresi, A. Rastelli, P. Alonso-González *et al.*, Nano Lett. **19**, 6931 (2019).

[45] D. Ziss, J. Martín-Sánchez, T. Lettner, A. Halilovic, G. Trevisi, R. Trotta, A. Rastelli, and J. Stangl, J. Appl. Phys. **121**, 135303 (2017).

[46] F. Ding, H. Ji, Y. Chen, A. Herklotz, K. Dörr, Y. Mei, A. Rastelli, and O. G. Schmidt, Nano Lett. **10**, 3453 (2010).

[47] M. M. Glazov, F. Dirnberger, V. M. Menon, T. Taniguchi, K. Watanabe, D. Bougeard, J. D. Ziegler, and A. Chernikov, Phys. Rev. B **106**, 125303 (2022).

[48] A. Dadgar, D. Scullion, K. Kang, D. Esposito, E. Yang, I. Herman, M. Pimenta, E.-J. Santos, and A. Pasupathy, Chem. Mater. **30**, 5148 (2018).

[49] L. Wang, S. Zihlmann, A. Baumgartner, J. Overbeck, K. Watanabe, T. Taniguchi, P. Makk, and C. Schonenberger, Nano Lett. **19**, 4097 (2019).

[50] F. Guan, P. Kumaravadivel, D. V. Averin, and X. Du, Appl. Phys. Lett. **107**, 193102 (2015).

[51] L. J. Wang, P. Makk, S. Zihlmann, A. Baumgartner, D. I. Indolese, K. Watanabe, T. Taniguchi, and C. Schönenberger, Phys. Rev. Lett. **124**, 157701 (2020).

[52] B. Aslan, M. Deng, and T. F. Heinz, Phys. Rev. B **98**, 115308 (2018).

[53] R. Frisenda, M. Drüppel, R. Schmidt, S. Michaelis de Vasconcellos, D. Perez de Lara, R. Bratschitsch, M. Rohlfing, and A. Castellanos-Gomez, npj 2D Mater. Appl. **1**, 10 (2017).

[54] Y. Y. Hui, X. Liu, W. Jie, N. Y. Chan, J. Hao, Y. T. Hsu, L. J. Li, W. Guo, and S. P. Lau, ACS Nano **7**, 7126 (2013).

[55] D. Edelberg, H. Kumar, V. Shenoy, H. Ochoa, and A. N. Pasupathy, Nat. Phys. **16**, 1097 (2020).

[56] J. Cenker, S. Sivakumar, K. Xie, A. Miller, P. Thijssen, Z. Liu, A. Dismukes, J. Fonseca, E. Anderson, X. Zhu, X. Roy, D. Xiao, J. H. Chu, T. Cao, and X. Xu, Nat. Nanotechnol. **17**, 256 (2022).

[57] P. Hernández López, S. Heeg, C. Schattauer, S. Kovalchuk, A. Kumar, D. J. Bock, J. N. Kirchhof, B. Höfer, K. Greben, D. Yagodkin *et al.*, Nat. Commun. **13**, 7691 (2022).

[58] S. Aas and C. Bulutay, Opt. Express **26**, 28672 (2018).

[59] S. Wang, M. S. Ukhtary, and R. Saito, Phys. Rev. Res. **2**, 033340 (2020).

[60] C. R. Zhu, G. Wang, B. L. Liu, X. Marie, X. F. Qiao, X. Zhang, X. X. Wu, H. Fan, P. H. Tan, T. Amand, and B. Urbaszek, Phys. Rev. B **88**, 121301(R) (2013).

[61] H. Zheng, B. Wu, S. Li, J. He, Z. Liu, C.-T. Wang, J.-T. Wang, J.-a. Duan, and Y. Liu, Opt. Lett. **48**, 2393 (2023).

[62] F. Li, M. J. Cabral, B. Xu, Z. Cheng, E. C. Dickey, J. M. LeBeau, J. Wang, J. Luo, S. Taylor, W. Hackenberger *et al.*, Science **364**, 264 (2019).

[63] A. Castellanos-Gomez, M. Buscema, R. Molenaar, V. Singh, L. Janssen, H. S. Van Der Zant, and G. A. Steele, 2D Mater. **1**, 011002 (2014).

[64] See Supplemental Material at http://link.aps.org/supplemental/10.1103/PhysRevB.108.L041404 for details on the performed experiments and calculations.

[65] X. Gao, J. Wu, Y. Yu, Z. Chu, H. Shi, and S. Dong, Adv. Funct. Mater. **28**, 1706895 (2018).

[66] Y. Chen, Y. Zhang, R. Keil, M. Zopf, F. Ding, and O. G. Schmidt, Nano Lett. **17**, 7864 (2017).

[67] J. Martín-Sánchez, R. Trotta, G. Piredda, C. Schimpf, G. Trevisi, L. Seravalli, P. Frigeri, S. Stroj, T. Lettner, M. Reindl *et al.*, Adv. Opt. Mater. **4**, 682 (2016).

[68] F. Cadiz, E. Courtade, C. Robert, G. Wang, Y. Shen, H. Cai, T. Taniguchi, K. Watanabe, H. Carrere, D. Lagarde *et al.*, Phys. Rev. X **7**, 021026 (2017).

[69] J. Wierzbowski, J. Klein, F. Sigger, C. Straubinger, M. Kremser, T. Taniguchi, K. Watanabe, U. Wurstbauer, A. W. Holleitner, M. Kaniber *et al.*, Sci. Rep. **7**, 12383 (2017).

[70] J. S. Ross, S. Wu, H. Yu, N. J. Ghimire, A. M. Jones, G. Aivazian, J. Yan, D. G. Mandrus, D. Xiao, W. Yao *et al.*, Nat. Commun. **4**, 1474 (2013).

[71] T. C. Berkelbach, M. S. Hybertsen, and D. R. Reichman, Phys. Rev. B **88**, 045318 (2013).

[72] G. D. Shepard, J. V. Ardelean, O. A. Ajayi, D. Rhodes, X. Zhu, J. C. Hone, and S. Strauf, ACS Nano **11**, 11550 (2017).

[73] Z. Li, T. Wang, S. Miao, Z. Lian, and S.-F. Shi, Nanophotonics **9**, 1811 (2020).

[74] P. Rivera, M. He, B. Kim, S. Liu, C. Rubio-Verdú, H. Moon, L. Mennel, D. A. Rhodes, H. Yu, T. Taniguchi *et al.*, Nat. Commun. **12**, 871 (2021).

[75] C. Robert, S. Park, F. Cadiz, L. Lombez, L. Ren, H. Tornatzky, A. Rowe, D. Paget, F. Sirotti, M. Yang *et al.*, Nat. Commun. **12**, 5455 (2021).

[76] M. Yang, L. Ren, C. Robert, D. Van Tuan, L. Lombez, B. Urbaszek, X. Marie, and H. Dery, Phys. Rev. B **105**, 085302 (2022).

[77] A. M. Jones, H. Yu, J. R. Schaibley, J. Yan, D. G. Mandrus, T. Taniguchi, K. Watanabe, H. Dery, W. Yao, and X. Xu, Nat. Phys. **12**, 323 (2016).

[78] K. Zollner, P. E. Faria Junior, and J. Fabian, Phys. Rev. B **100**, 195126 (2019).

[79] D. Huang, K. Sampson, Y. Ni, Z. Liu, D. Liang, K. Watanabe, T. Taniguchi, H. Li, E. Martin, J. Levinsen, M. M. Parish, E. Tutuc, D. K. Efimkin, and X. Li, Phys. Rev. X **13**, 011029 (2023).

[80] J. P. Perdew, A. Ruzsinszky, G. I. Csonka, O. A. Vydrov, G. E. Scuseria, L. A. Constantin, X. Zhou, and K. Burke, Phys. Rev. Lett. **100**, 136406 (2008).

[81] D. J. Singh and L. Nordstrom, *Planewaves, Pseudopotentials, and the LAPW Method* (Springer, Berlin, 2006).

[82] P. Blaha, K. Schwarz, F. Tran, R. Laskowski, G. K. Madsen, and L. D. Marks, J. Chem. Phys. **152**, 074101 (2020).

[83] S. R. Bahn and K. W. Jacobsen, Comput. Sci. Eng. **4**, 56 (2002).

[84] P. E. Faria Junior, K. Zollner, T. Woźniak, M. Kurpas, M. Gmitra, and J. Fabian, New J. Phys. **24**, 083004 (2022).

[85] F. Dirnberger, J. D. Ziegler, P. E. Faria Junior, R. Bushati, T. Taniguchi, K. Watanabe, J. Fabian, D. Bougeard, A. Chernikov, and V. M. Menon, Sci. Adv. **7**, eabj3066 (2021).

[86] M. He, P. Rivera, D. Van Tuan, N. P. Wilson, M. Yang, T. Taniguchi, K. Watanabe, J. Yan, D. G. Mandrus, H. Yu *et al.*, Nat. Commun. **11**, 618 (2020).
[87] H. Tornatzky, A.-M. Kaulitz, and J. Maultzsch, Phys. Rev. Lett. **121**, 167401 (2018).
[88] G. Kioseoglou, A. T. Hanbicki, M. Currie, A. L. Friedman, and B. T. Jonker, Sci. Rep. **6**, 25041 (2016).
[89] M. M. Glazov, T. Amand, X. Marie, D. Lagarde, L. Bouet, and B. Urbaszek, Phys. Rev. B **89**, 201302(R) (2014).
[90] V. Shahnazaryan, I. Iorsh, I. A. Shelykh, and O. Kyriienko, Phys. Rev. B **96**, 115409 (2017).
[91] O. Kyriienko, D. Krizhanovskii, and I. Shelykh, Phys. Rev. Lett. **125**, 197402 (2020).
[92] R. Perea-Causin, S. Brem, and E. Malic, Phys. Rev. B **106**, 115407 (2022).
[93] J. Klein, M. Florian, A. Hötger, A. Steinhoff, A. Delhomme, T. Taniguchi, K. Watanabe, F. Jahnke, A. W. Holleitner, M. Potemski, C. Faugeras, A. V. Stier, and J. J. Finley, Phys. Rev. B **105**, L041302 (2022).